Thermal analysis of a miniature magnetic fluid seal installed in an implantable rotary pump

Yoshinori Mitamura[a], Ikuya Nishimura[a], Tetsuya Yano[b]

Yoshinori Mitamura
[a]Graduate School of Information Science and Technology, Hokkaido University, Kita 14-jo Nishi 9-chome, Kita-ku, Sapporo 060-0814, Japan
Email: ymitamura@par.odn.ne.jp

Ikuya Nishimura
[a]Graduate School of Information Science and Technology, Hokkaido University, Kita 14-jo Nishi 9-chome, Kita-ku, Sapporo 060-0814, Japan
Email: mura@ist.hokudai.ac.jp

Tetsuya Yano
[b]Faculty of Science and Technology, Hirosaki University, 3 Bunkyo-cho, Hirosaki-shi, Aomori-ken 036-8560, Japan
Email: yano@hirosaki-u.ac.jp

Corresponding author
Yoshinori Mitamura
5-5-1-2 Sumikawa, Minami-ku, Sapporo 005-0005, Japan
Email: ymitamura@par.odn.ne.jp

Abstract

The capacity of a magnetic fluid (MF) seal is decreased by increased MF temperature. A cooling system for MF is limited in a miniature MF seal installed in an implantable rotary pump. MF temperature in an MF seal installed in an implantable rotary pump was studied.

The temperature of MF in a rotary pump was measured in vitro. Also, steady-state thermal analyses were conducted for an implantable rotary pump model. The results showed that (1) the decrease in magnetization of an MF due to increased temperature is negligible when the heat transfer coefficient of the seal housing is greater than 500 W/(m^2·K) and (2) the increased temperature is mainly due to heat flux from the motor, and the magnitude of temperature increase due to viscous friction in the MF is low.

In conclusion, an MF seal can be used in an implantable rotary pump from the standpoint of heat characteristics.

Keywords: magnetic fluid seal, thermal analysis, temperature, implantable medical device

1. Introduction

A magnetic fluid (MF) seal enables mechanical contact-free rotation of a shaft and hence has excellent durability. The life of a conventional MF seal, however, decreases in liquids. MF seals used in our previous study failed after 6 days and 11 days [1]. Factors limiting seal life are MF flowing away and mixing of MF with liquids. To overcome these problems, we developed an MF seal that had a "shield" mechanism. The use of an optimally designed shield prolonged an MF seal life for more than 207 days, while the MF seal with a conventional shield failed after about 30 days [2]. Based on these results, we are planning to install the MF seal in an implantable rotary pump.

Temperature rise of MF in an MF seal is induced by viscous friction in the MF. MF temperature rise should be controlled because it decreases the seal capacity and causes evaporation of the MF. The influence of temperature on the sealing performance of the rotating MF seal has been studied. The maximum temperature of an MF on the surface of a hermetically sealed shaft under isothermal boundary conditions was calculated by using a one-dimensional approximation model [3]. The pressure-resistance capacity of a large-diameter MF seal decreased at high temperatures and increased with decrease in temperature at 0 ℃~ -55 ℃ [4]. The starting torque of the rotating MF seal was low in the temperature range of 25 ℃~70 ℃ and it increased with decrease in temperature due to increase of viscosity at -55 ℃~ -25 ℃ [5]. Steady-state thermal analysis was conducted to obtain the temperature of the MF seal by using the finite volume method [6]. Boundary conditions of the model were

the natural convection heat transfer wall surface and the forced convection heat transfer cooling channel wall surface. The sealing pressure was obtained with consideration of the influence of MF temperature. The simulation and experimental results showed that the sealing capacity decreased with increase in rotational speed. For a static MF seal, heating of the MF seal was found to be an effective method for homogenizing the MF in the seal [7].

In previous studies, the influence of temperature changes caused by high rotational speeds, a large-diameter MF seal or environment temperature was mainly investigated. However, cooling conditions of an MF seal to control the MF temperature have rarely been studied. MF temperature is determined by the balance between the heat generation and diffusion. In industrial applications of an MF seal various cooling systems can be used. In an implantable rotary pump, however, the use of a cooling system is limited.

The objective of this study was to investigate MF temperature in an MF seal installed in an implantable rotary pump and to determine the cooling conditions for controlling MF temperature within a permissible range.

2. Methods

2.1 Miniature MF seal

The MF seal consisted of a magnet (Nd-Fe-B magnet, Hc: 876 kA/m, Br: 1.26 T, outer diameter (OD): Φ4 mm, inner diameter (ID): Φ2mm, L: 1 mm) sandwiched by asymmetric trapezoidal pole pieces (SUS420, OD: Φ4 mm, ID: Φ1.1 mm, L: 0.5 mm) (Figure 1). The MF

seal was installed on a rotating shaft (Φ1.0 mm) of a motor. The gap between the pole piece and the shaft was 50 μm. The gap was filled with MF (Ferrotec, Exp.15067) specially developed for this seal. The new MF (Exp.15067) has a high saturated magnetization of 47.9 kA/m, a high viscosity of 0.5 Pa·s and a density of 1.390 g/cc. The shield was made of a nonmagnetic material (SUS303). The gap between the shield and the shaft was 100 μm.

2. 2 Temperature measurement of the MF seal installed in a rotary pump

A rotary pump in which the miniature MF seal was installed was connected to a reservoir through a flowmeter (BBBC4168, TOFCO Corp. Tokyo, Japan) by silicone tubes (Figure 2). The pump was placed on the floor and the reservoir was hung at 136 cm above the floor. The circuit was filled with distilled water. Pump flow rate was stepwise changed from 0.5 L/min to 1.0 and 1.5 L/min. A T-type thermocouple (Φ1 mm) was inserted in the vicinity of the MF seal (1.5 mm from MF) through an exhaust port and the temperature was measured by a data logger thermometer (Center 520, Center Technology, Taiwan). Room temperature was also measured by the thermocouple. Motor speed, voltage and current were measured.

2.3 Steady-state thermal analyses

2.3.1 Rotary pump model

An analysis model consisted of an MF seal, a seal housing, a motor housing, and a motor (Figure 3). A pump housing and an impeller were excluded from the rotary pump model.

Thermal conductivity of materials used in the analysis is shown in Table 1.

Two heat sources, a motor and MF, were used in the analysis model. Heat loss of the motor was calculated by (coil resistance) × (motor current)^2.

Heat generation due to viscous friction in the MF was calculated as follows. MF in the gap between the pole piece tooth and the motor shaft is shown in Figure 4. Assuming that the MF flow is laminar and that the speed distribution in each axial section is linear, heat release in the MF due to viscous friction is given by

$$W = \mu \cdot \frac{R\omega}{z} \cdot 2\pi R \cdot t_1 \cdot R\omega + \mu \int_0^{t_2} \frac{R\omega}{x+z} \cdot 2\pi R \cdot R\omega \, dx$$

$$= 2\pi R^3 \omega^2 \mu \left(\frac{t_1}{z} + \ln \frac{z+t_2}{z}\right), \qquad \text{(equation 1)}$$

where R is the radius of the shaft (0.5 mm), ω is angular velocity of the shaft, μ is viscosity of the MF (0.5 Pa·s), t_1 is length of the pole piece tooth tip (0.1 mm), t_2 is half length of the pole piece (0.2 mm) and z is the gap between the pole piece and shaft (0.05 mm) [8].

Temperature in the rotary pump model is obtained by solving the following cylindrical coordinates diffusion equation:

$$\frac{\kappa}{r}\frac{\partial}{\partial r}\left(r\frac{\partial T}{\partial r}\right) + \frac{\kappa}{r^2}\frac{\partial^2 T}{\partial \theta^2} + \kappa\frac{\partial^2 T}{\partial z^2} + Q = 0,$$

where T is temperature, κ is thermal conductivity and Q is heat per unit volume. The heat diffusion equation was solved by using an FEM. An element shape was a second order quadratic hexahedron. The element was defined by 20 nodes with a temperature degree of freedom at each node. The maximum element sizes were limited to 0.03 mm in the MF region, 0.5 mm in the exhaust port region and 0.2 mm in the motor region. The numbers of elements

were 29,246 in the rotary pump model, 24,942 in the basic model of an MF seal and 25,295 in the catheter-type pump model. Steady-state thermal analyses were performed using ANSYS Workbench 2021-R1 Academic (ANSYS, Inc.) under the following two conditions.

(1) The same motor driving conditions as those in the pump experiments (Figure 2) were used. They were a motor input power of 0.6 W (motor speed: 12,800 rpm), 1.8 W (motor speed: 20,900 rpm) or 3.78 W (motor speed: 28,100 rpm) and a room temperature of 25 ℃ and a motor input power of 0.6 W, 1.8 W or 3.66 W (motor speed: 27,800 rpm) and a room temperature of 26 ℃.

(2) Three different combinations of heat sources were used: (a) two heat sources of a motor (3.78 W) and MF (shaft rotational speed of 28,100 rpm), (b) one heat source of a motor (3.78 W) and (c) one heat source of MF (shaft rotational speed of 28,100 rpm).

Boundary conditions were set as follows. Thermal transfer coefficients were 1500 W/m^2·K for the surfaces in contact with water and 25 W/m^2·K for the surfaces in contact with air. Ambient temperature was set at 25 ℃. The thermal transfer coefficient of 1500 W/(m^2·K) was used with reference to the coefficient for forced convection of water on a flat plate. The thermal transfer coefficient of air for natural convection is reported to be 2-25 W/(m^2·K), and 25 W/(m^2·K) was therefore used in this study.

2.3.2 Basic model of an MF seal

Thermal analysis was performed for a magnetic seal basic model (Figure 5). The structure of the seal is the same as that shown in Figure 1. The seal housing is a cylinder with an outer

diameter of 8.5 mm, an inner diameter of 4 mm and a length of 3.5 mm. The material of the seal housing is titanium (thermal conductivity: 21.9 W/m·K). The heat source is MF. Heat release from the MF was given by equation (1). Boundary conditions were given as follows. A thermal insulation condition was applied to the surfaces facing the motor. The heat transfer coefficient of other surfaces in contact with blood was changed from 25 to 500 $W/m^2 \cdot K$. Ambient temperature was set at 37 ℃.

2.3.3 MF seal in a catheter-type pump

A model of a catheter pump consists of a motor, an MF seal, and a housing (Figure 6). An impeller is excluded. The structure of the MF seal is the same as that shown in Figure 1. The motor and MF seal assembly are encased in a titanium housing (OD: Φ.8.5 mm and L: 37 mm).

Two heat sources, the motor and the MF, were used. Motor heat loss was set at 0.284 W and motor speed was set at 20,000 rpm (rated speed). Boundary conditions were as follows. The heat transfer coefficient of all surfaces was changed from 25 to 500 $W/m^{2\cdot}K$ and ambient temperature was kept at 37 ℃.

3. Results

3.1 Temperature measurement of the MF seal installed in the rotary pump

Changes in temperature in the exhaust port are shown in Figure 7. The temperature reached a steady state after about 20 minutes. Temperature increases from room temperature were 0.3 ℃ and 0.4 ℃ for a motor input power of 0.6 W, 0.9 ℃ and 1.3 ℃ for a motor input

power of 1.8 W, 2 ℃ for a motor input power of 3.78 W and 2.6 ℃ for a motor input power of 3.66 W.

3.2 Steady-state thermal analysis of the MF seal in the rotary pump

(1) Temperatures in the exhaust port for different motor input powers are shown in Figure 8. The relationship between computed and measured temperatures in the exhaust port is shown in Figure 9. A good correlation was obtained between the computed and measured temperatures.

(2) Computed MF temperatures for three different heat sources are shown in Table 2. The results indicate that the MF temperature increase from the ambient temperature with two heat sources (motor and MF) is obtained by summation of the temperature increase for each heat source (motor or MF). More importantly, the temperature increase of MF in the seal installed in the rotary pump was mainly due to the heat flux from the motor. Therefore, it is difficult to reveal the temperature increase of MF due to the viscous friction in the MF by experiments. Thermal analysis of an MF seal is important because it can exclude the influence of heat flux from the motor.

3.3 Steady-state thermal analysis of a basic model of the MF seal

Temperature distribution on a cross section of the seal is shown in Figure 10 for a shaft rotational speed of 20,000 rpm and a heat transfer coefficient of 500 $W/m^2 \cdot K$. The

temperature of the MF was 37.95 ℃. The relationship between MF temperature and boundary condition (heat transfer coefficient) at different shaft rotational speeds is shown in Figure 11. MF temperature increased with increase in rotational speed of the shaft. MF temperature was almost the same for a heat transfer coefficient higher than 300 W/m^2·K.

3.4 Steady-state thermal analysis of an MF seal in a catheter-type pump

The temperature distribution on a cross section of the seal assembly with a heat transfer coefficient of 500 W/m^2·K under the condition of a blood temperature of 37 ℃ is shown in Figure 12. The MF temperature was 37.7 ℃. The relationships between MF temperature and heat transfer coefficients of surfaces in contact with blood are shown in Figure 13. Two heat source models were used. One was a motor and MF model and the other one was an MF model. The temperature difference between the two models is due to the influence of heat flux from the motor. The influence of heat source from the motor is negligible in heat transfer coefficients above 400 W/m^2·K.

4. Discussion

It is well known that magnetization of a magnetic material decreases with an increase of temperature. Magnetization of an MF also decreases with increase of temperature. This leads to a decrease of seal capacity. It is therefore important to investigate the temperatures of MF in MF seals, especially in high-speed MF seals [9-11].

The temperature of MF is determined by the balance between heat generation in the MF and heat diffusion from the MF to surrounding materials. Heat generation due to viscous friction in the MF is given by equation (1). At a motor speed of 20,000 rpm, heat generation is 2.08×10^8 W/m^3 in a cylinder-shaped MF (0.55 mm in OD, 0.5 mm in ID and 0.1 mm in L) and it is 2.41×10^7 W/m^3 in a hollow truncated cone-shaped MF (an upper surface of 0.55 mm in D, a lower surface of 0.75 mm in D and length of 9.2 mm with a hollow of 0.5 mm in D) (Figure 4). Volume, weight, surface area and heat capacity of the MFs are shown in Table 3. Specific heat capacity of the MF is 1960 J/(Kg·K). As shown in Table 3, temperature of the cylinder-shaped MF increases at a rate of 76.4 K/s and temperature of the hollow truncated cone- shaped MF increases at a rate of 8.52 K/s in a thermal insulation condition. In an actual MF seal in a rotary pump, the heat generated in the MF diffuses into a fluid flowing on the surface of seal housing through the seal housing and the motor shaft. Since the temperature of MF is determined by the balance between heat generation and diffusion, the heat diffusion equation was solved by using an FEM analysis.

A steady-state thermal analysis of the MF seal in a rotary pump was performed (Figure 8). Two heat sources, a motor and MF, were included in the pump model. Comparison of the computed and measured temperatures showed that the computed temperature is reliable (Figure 9). The effects of the two heat sources on MF temperature were independently analyzed (Table 2). The increase of MF temperature was mainly due to the motor in the rotary pump. Therefore, steady-state thermal analysis of a basic model of the MF seal (Figure 5) was

conducted to investigate the temperature rise of the MF due to viscous friction in the MF alone. A thermal insulation condition was applied to the seal surfaces facing the motor. The MF temperature rise from body temperature was 0.95 ˚C (T=37.95 ˚C) at a shaft rotational speed of 20,000 rpm and a heat transfer coefficient of 500 W/(m^2·K) (Figure 11). MF temperature decreased with increase in the heat transfer coefficient of the seal housing surface. MF temperature was almost constant for heat transfer coefficients higher than 300 W/(m^2·K). MF temperature was 39.4 ˚C (△T=2.4 ˚C) at 30,000 rpm (maximum pump speed) with a heat transfer coefficient of 300 W/(m^2·K).

A relationship between magnetization and temperature of an MF at a low magnetic field (about 8 kA/m) has been reported [12, 13]. At a high magnetic field (about 800 kA/m), the relationship between magnetization and temperature of magnetite particles was measured. Relative magnetization (M/M_S) between 20 ˚C and 100 ˚C is approximated by the following equation:

$$M/M_S = -0.0009 \cdot T(^{\circ}C) + 1.0195,$$

where M_S is saturation magnetization at a temperature of 20 ºC and M is saturation magnetization at a temperature T ºC. If the density of an MF is constant, magnetization of the MF decreases by 1.3% at 37.95 ˚C and 1.5% at 39.4 ˚C from the magnetization at room temperature (25 ˚C). Therefore, the decrease of seal capacity due to increased MF temperature caused by viscous friction is negligible at conventional shaft speeds when the heat transfer coefficient is higher than 500 W/(m^2·K) on the seal housing surfaces.

Steady-state thermal analysis of the MF seal in a catheter-type pump showed that MF temperature was 37.7 ℃ at a shaft speed of 20,000 rpm and a heat transfer coefficient of 500 W/(m^2·K) on all pump surfaces (Figure 12). The total surface area of the catheter-type pump is 1.1×10^{-3} m^2 and motor heat loss is 0.284 W. Therefore, the temperature difference between the pump surface and blood is 0.52 ℃. Decrease of magnetization at 37.7 ℃ is 1%. Therefore, decrease in the capacity of the MF seal in a catheter-type pump due to increased MF temperature is negligible when the heat transfer coefficient of pump surfaces is higher than 500 W/(m^2·K) .

There are limitations in this study. The energy dissipation magnitude is determined by the velocity field distribution in an MF volume. The azimuthal component of the velocity gives the main contribution to energy dissipation in the ring-shaped MF layer. However, influence of transverse flow on the energy dissipation becomes essential with increasing rotational speed of the inner shaft [14]. In this study, the energy dissipation was given with the assumption that only the azimuthal component of the velocity contributed to the heat generation. If the rotational speed of the shaft increases more, the influence of transverse flow will have to be considered.

Viscous friction was calculated with the assumption of constant MF viscosity. However, viscosity of MF decreases with an increase of MF temperature. Therefore, heat generation due to viscous friction in the MF was slightly overestimated in this study. However, if the rotational speed increases more and the influence of transverse flow on the energy dissipation

becomes essential, heat generation calculated by equation 1 might be underestimated.

The heat source model of a motor was simple. Heat loss of a motor was calculated by (coil resistance) × (motor current)^2. The heat source was assumed to be distributed uniformly inside the motor. However, the motor coil is located in a certain place inside the motor. A more precise motor model would be preferable, but steady-state thermal analysis using the simple motor model gave a temperature close to the measured temperature (Figure 9). Also, the objective of this study was to investigate the MF temperature rise due to viscous friction in the MF with consideration of heat diffusion through the seal housing. Although the MF temperature increased mainly due to heat flux from the motor, this does not have any relation to the design of an MF seal. It is important to design a rotary pump to release heat from the motor efficiently, but this is another subject of a future study.

5. Conclusions

1. The capacity of a miniature MF seal installed in an implantable rotary pump is not impaired by MF temperature rise due to viscous friction when the heat transfer coefficient of the seal housing is greater than 500 W/(m^2·K).

2. MF temperature of an MF seal installed in a rotary pump is affected by heat flux from the motor. It is important to design a rotary pump to decrease the thermal influence of the motor on an MF seal.

3. A miniature MF seal can be used in an implantable rotary pump in consideration of its

heat characteristics.

This research did not receive any specific grant from funding agencies in the public, commercial, or not-for-profit sectors.

References

[1] Y. Mitamura, S. Takahashi, S. Amari, E. Okamoto, S. Murabayashi, I. Nishimura, A magnetic fluid seal for rotary blood pumps: effects of seal structure on long-term performance in liquid, J Artif Organs 14 (2011) 23–30, https://doi.org/10.1007/s10047-010-0526-8.

[2] Y. Mitamura, K. Sekine, E. Okamoto, Magnetic fluid seals working in liquid environments: Factors limiting their life and solution methods, J. Magn. Magn. Mater. 500 (2020), 166293, https://doi.org/10.1016/j.jmmm.2019.166293.

[3] L. P. Orlov, A. K. Sinitsyn, V. E. Fertman, Effect of heat transfer on the limiting characteristics of magnetofluid seals, J. Eng. Phys. 42 (1982) 46-52.

[4] D. Hao, D. Li, J. Chen, J. Yu, Theoretical analysis and experimental study of the characteristics of magnetic fluid seal with a large diameter at high/low temperatures, Int. J. Appl. Electromagn. Mech. 58(2018) 531-550, https://doi.org/10.3233/JAE-180065.

[5] J. Chen, D. Li, D. Hao, Investigation on the influence of temperature on starting torque of magnetic fluid seal. J. Magn. 23(2018) 436-441, https://doi.org/10.4283/JMAG.2018.23.3.436.

[6] Y. Chen 1, D. Li, Y. Zhang, Z. Li, H. Zhou, The influence of the temperature rise on the sealing performance of the rotating magnetic fluid seal, IEEE Trans on Magnetics 56 (2020)

4600510, https://doi.org/10.1109/TMAG.2020.3023018.

[7] M.S. Krakov, L.V. Nikiforov, Regarding the influence of heating and the Soret effect on a magnetic fluid seal, J. Magn. Magn. Mater. 431(2017) 255-261, http://dx.doi.org/10.1016/j.jmmm.2016.07.054.

[8] B.M. Berkovsky, V.F. Medvedev, M.S. Krakov, Magnetic Fluids: Engineering Applications, Oxford University Press, Oxford, 1993, p. 137.

[9] V.E Fertman, Heat dissipation in high-speed magnetic fluid shaft seal, IEEE Trans on Magnetics MAG-16 (1980) 352-357.

[10] M.O. Lutset, V. A. Starovoitov, Experimental studies of high-speed cryogenic magnetic fluid seals, IEEE Trans on Magnetics MAG-16 (1980) 343-346,

[11] V.K. Rakhuba, V.B. Samoilov, V.A. Chernobai, Dynamics of high-speed magnetic fluids seals, J. Magn. Magn. Mater. 39 (1983) 152-154,

[12] A. E. Virden, K. O'Gradya, The temperature dependence of magnetization in ferrofluids, J Appl Physics 99 (2006) 08S106, DOI: 10.1063/1.2172892

[13] Y. Dikansky, A. Ispiryan, S. Kunikin, On the temperature dependence of ferrofluid susceptibility, EPJ Web of Conferences 185, 09011 (2018),

https://doi.org/10.1051/epjconf/201818509011

[14] B.M. Berkovsky, M.S. Krakov, S.G. Pogirnitskaya, Influence of axisymmetric flow structure on energy dissipation in a ring-shaped layer of magnetic fluid, J. Magn. Magn. Mater. 149 (1995) 101-103, DOI10.1016/0304-8853(95)00347-9.

Table 1 Thermal conductivity of materials

Material	Thermal conductivity (W/m・K)	Remarks
Air	0.0256	
Aluminum alloy	150	
Magnet	8.95	
MF	0.15	
SUS303	15	Shield
SUS420	25	Motor, Pole piece

Table 2 Estimation of MF temperatures

Heat source			
Motor ($W/m^{3)}$	2.07×10^{6}	2.07×10^{6}	0
MF (W/m^{3})	4.75×10^{7} & 4.10×10^{8}	0	4.75×10^{7} & 4.10×10^{8}
Temperature of MF (℃)	28.72	27.86	25.92
Temperature increase from room temperature (℃)	3.72	2.86	0.92

Table 3 Physical values of MFs at a motor speed of 20,000 rpm

MF	Heat generation (W)	Volume (m^3)	Weight (Kg)	Surface area (m^2)	Heat capacity (J/K)
Cylinder-shaped MF	3.43×10^{-3}	1.65×10^{-11}	2.29×10^{-8}	9.89×10^{-7}	4.49×10^{-5}
Hollow truncated cone-shaped MF	2.77×10^{-3}	1.15×10^{-10}	1.66×10^{-7}	6.93×10^{-4}	3.25×10^{-4}

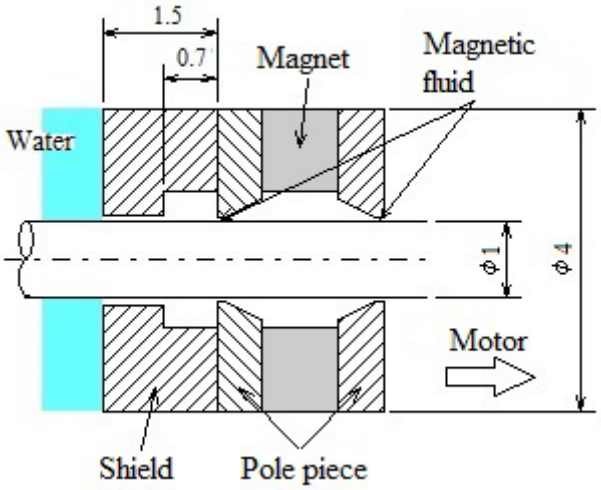

Figure 1 Miniature MF seal.

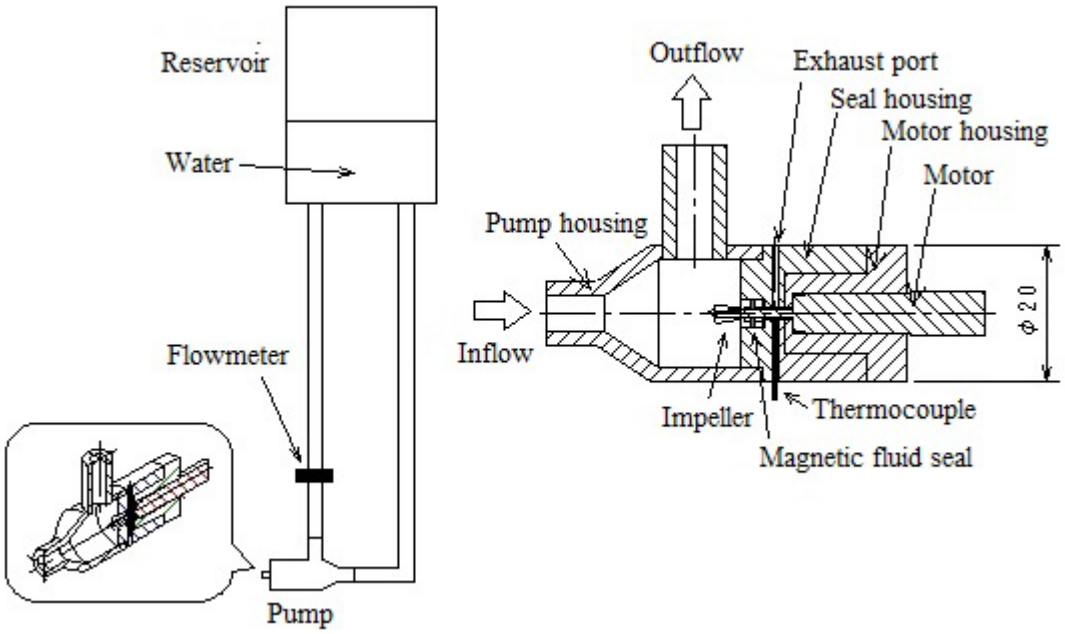

Figure 2 Experimental setup for temperature measurement of an MF seal installed in a rotary pump.

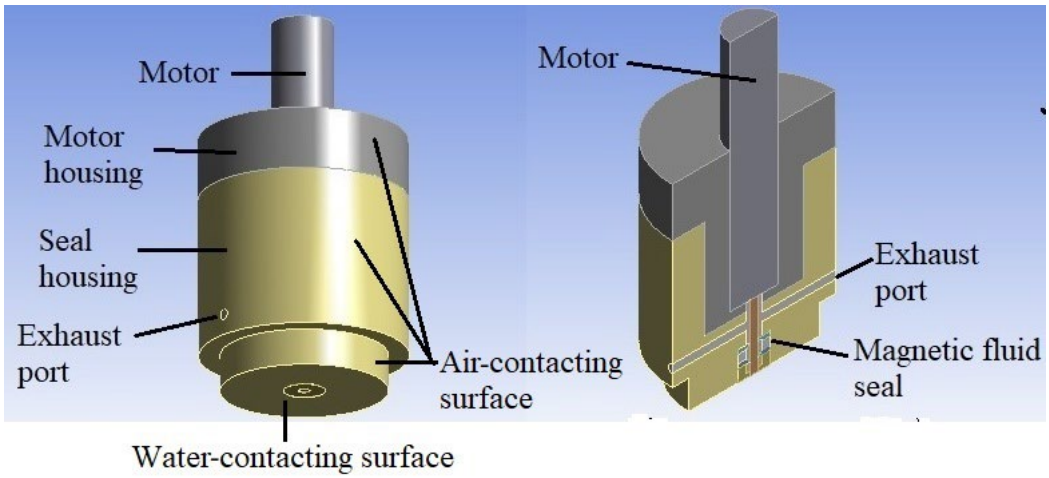

Figure 3 Analysis model of the MF seal in the rotary pump.

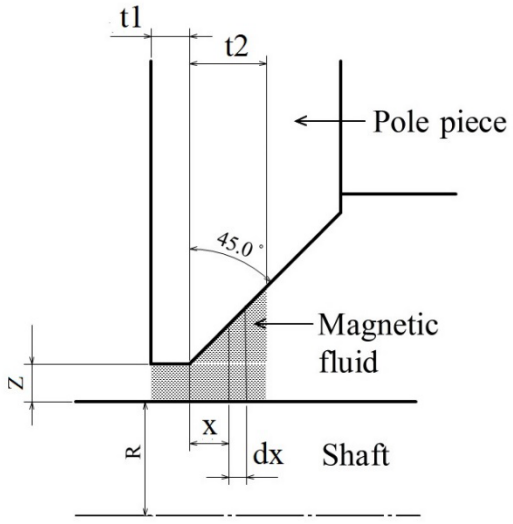

Figure 4 MF in the seal.

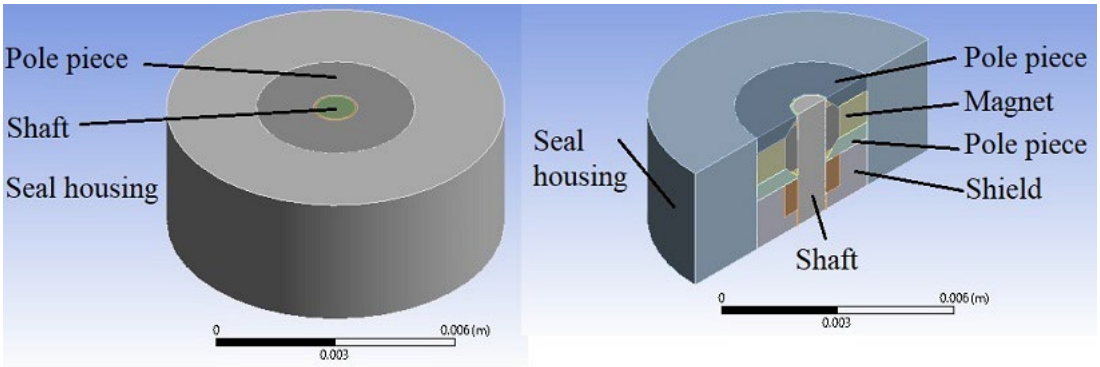

Figure 5 Basic model of an MF seal.

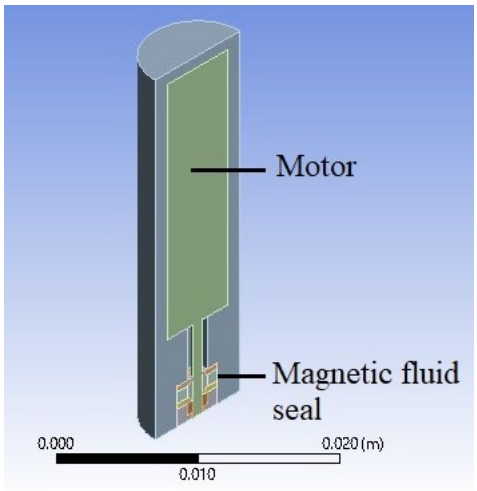

Figure 6 MF seal in a catheter-type pump.

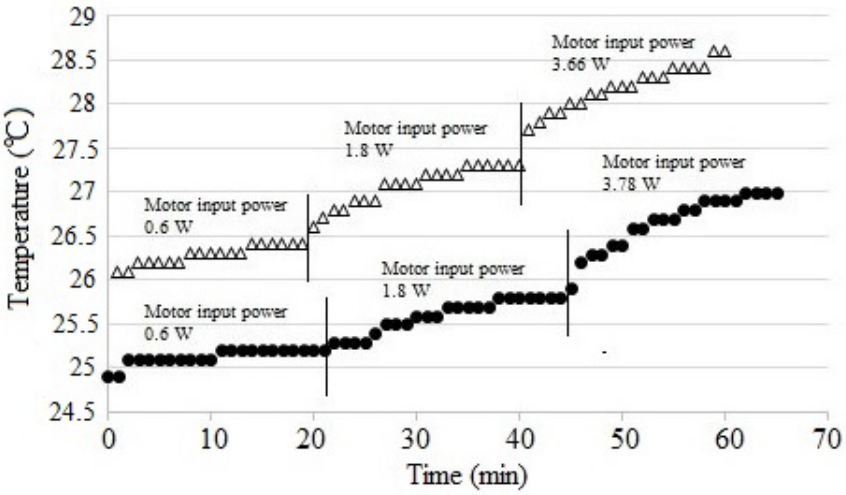

Figure 7 Changes in temperature in the exhaust port.

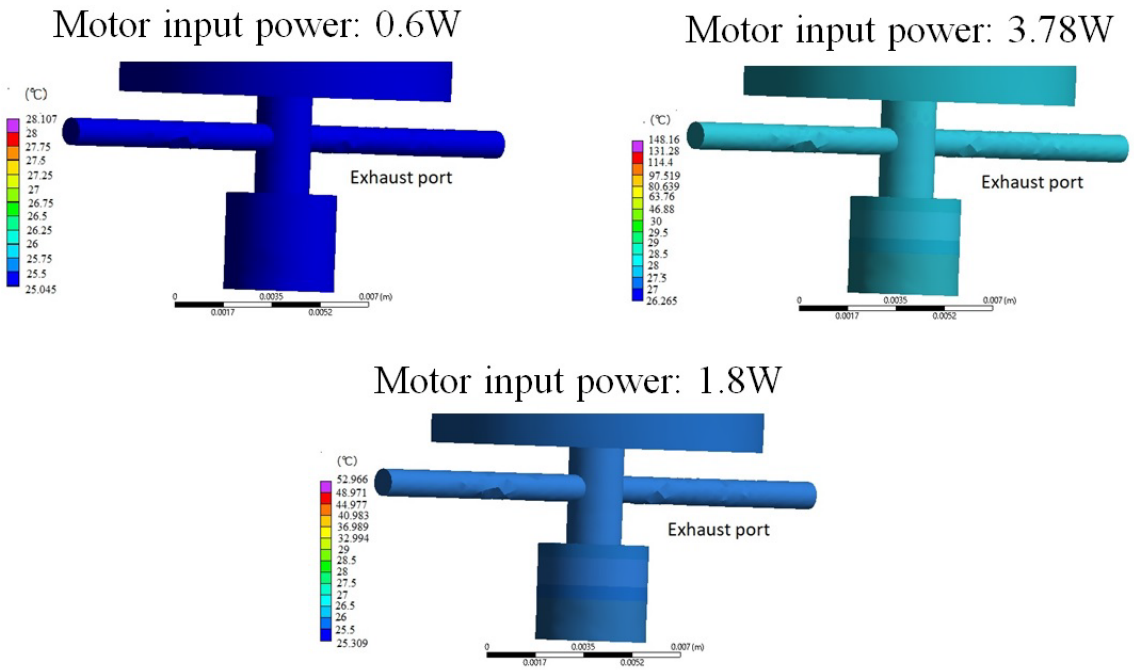

Figure 8 Temperatures in the exhaust port for different motor input powers. A seal housing is not shown.

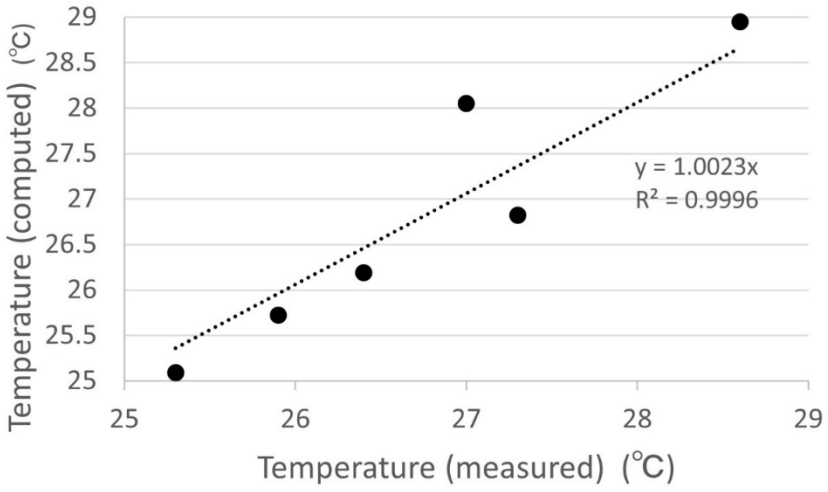

Figure 9 Relationship between computed and measured temperatures.

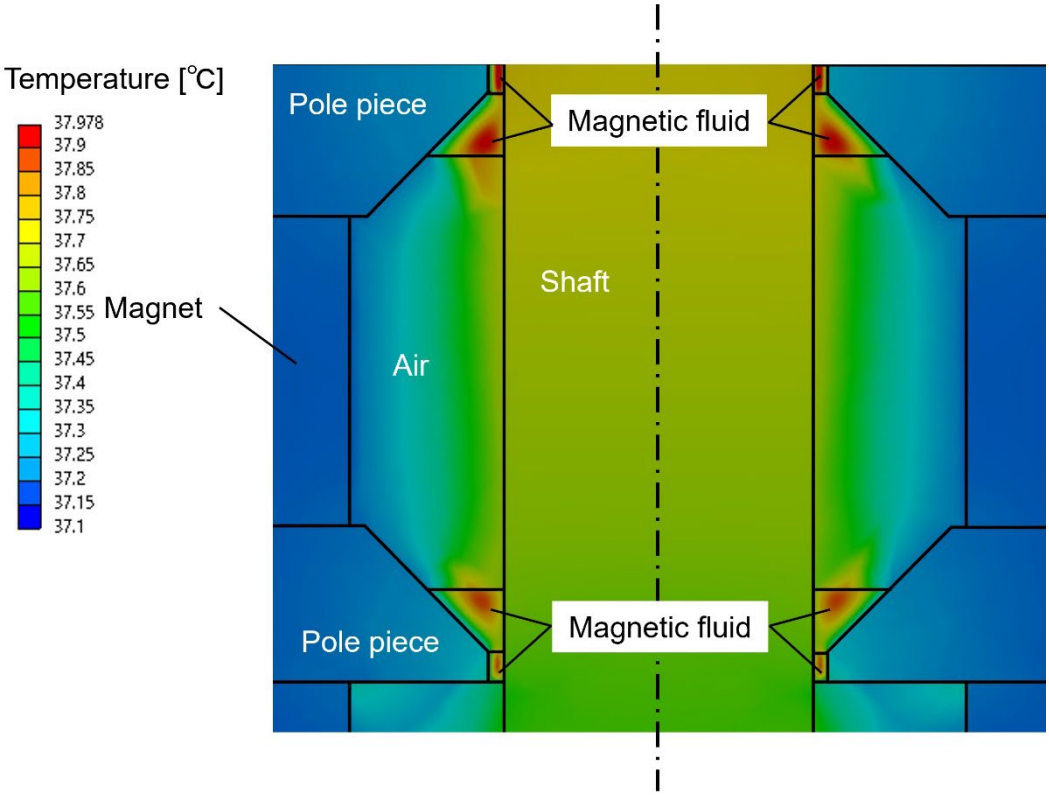

Figure 10 Temperature distribution in MF of a basic MF seal model.

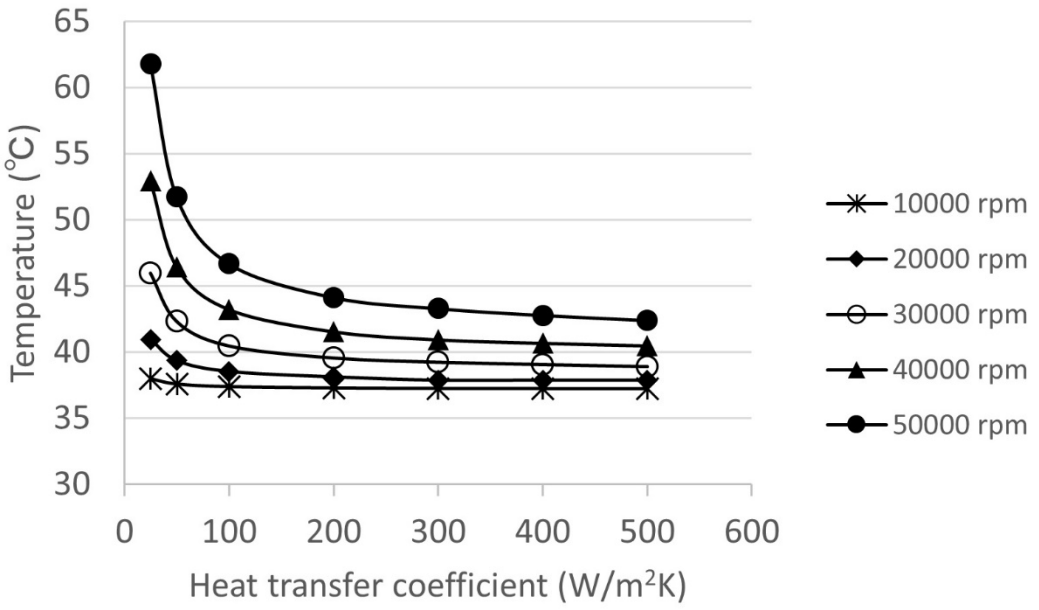

Figure 11 Relationship between MF temperature and heat transfer coefficient of the pump housing for different motor speeds.

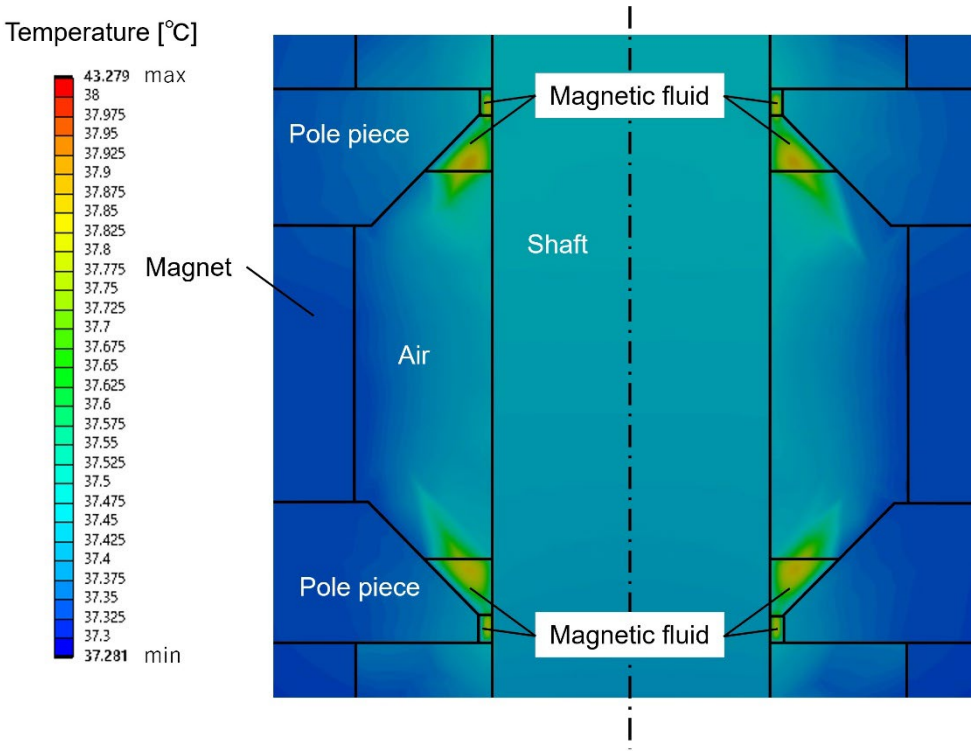

Figure 12 Temperature distribution in the MF seal of a catheter-type pump model.

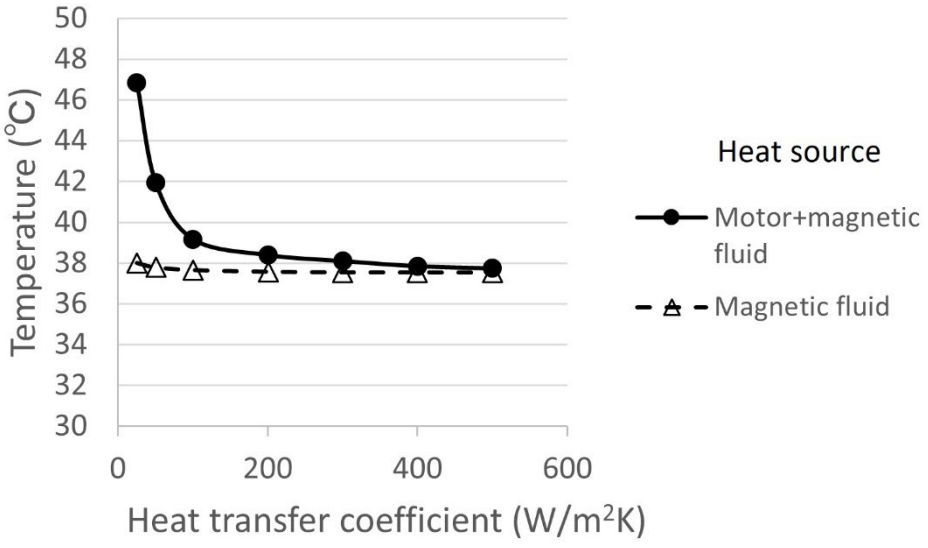

Figure 13 MF temperature in the catheter-type pump model for two different heat source models.